Uncertainty Evaluation in Multi-State Physics Based Aging Assessment of Passive Components

Askin Guler[a,*], Tunc Aldemir[a], and Richard Denning[a]
[a] Nuclear Engineering Program
The Ohio State University, Columbus, OH, USA

Abstract:

A methodology is presented to evaluate aging degradation of passive components under uncertainty. Stress corrosion cracking (SCC) degradation is selected as the example aging phenomenon and the methodology is implemented on the pressurizer surge line pipe weld of a pressurized water reactor. The degradation is described as a multi-state model consisting of six differential equations with system history dependent transition rates. The input data to the model include operating temperature, weld residual stress, stress intensity factor, thermal activation energy for crack initiation and crack growth. The associated uncertainties are represented by probability distributions derived from historical data, experimental data, expert elicitation, physics, or a combination of these. Latin Hypercube Sampling is used to generate observations from the distributions governing these parameters with a two-step approach that distinguishes between aleatory and epistemic uncertainties. The degradation model is solved by a semi-Markov approach using the concept of sojourn time to account for system history dependence of transition rates. The results are compared to a single step sampling process. The results show highest sensitivity of damage to weld residual stress.

Keywords: Aging, Passive components, LHS, semi-Markov, Uncertainty analysis

1. INTRODUCTION

Long term reliability of systems, structures and components (SSCs) in the existing fleet of operating reactors should be ensured to prevent a reduction in component and system safety margins due to aging. In order to address multiple aging mechanisms involving large numbers of components (with possibly statistically dependent failures) in a computationally feasible manner, a methodology is being developed where the sequencing of events leading to damage is conditioned on the physical conditions predicted in a simulation environment [1].

A state transition model [2] was selected as a case-study to implement the methodology. This model is applied to the pressurizer surge line pipe weld of a pressurized water reactor (PWR) to model primary water stress corrosion cracking (PWSCC) degradation during extended operation life (80 years) of the plant. The degradation model described in this paper was originally developed in [2] and later improved by using the sojourn time approach [3] with operational history-dependent transition rates [4]. The model has many input parameters including temperature, weld residual stress, stress intensity factor, and thermal activation energy for crack initiation and crack growth. The associated uncertainties are represented by probability distributions derived from historical data, experimental data, expert elicitation, physics, or a combination of these. The model output is pipe rupture probability as a function of operating time.

Although the separation of uncertainties as aleatory versus epistemic can be subjective, it can be helpful in supporting decision-making. In this paper, the uncertainty in the PWSCC model (Section 2) input is propagated using Latin hypercube sampling (LHS) while distinguishing between the aleatory

* guler.11@osu.edu

and epistemic uncertainties (Section 3). The results are compared to a single step approach that does not make such a distinction (Section 3.1). A sensitivity analysis is performed using the response surface methodology (RSM) to identify the most important model parameter that affects the rupture probability (Section 3.2). Conclusions of the study are given in Section 4.

2. THE MULTI-STATE SEMI-MARKOV MODEL

The state transition model to predict piping system reliability that is used in the paper was originally proposed by Fleming [5] and later adapted for system history dependent transition rates by Unwin et al. [2]. This 6-state state transition model is implemented for a PWR pressurizer surge line pipe weld (Alloy 182) for the case of a PWSCC scenario. Section 2.1 describes the model and Section 2.2 describes the procedure that is used to convert the model to a semi-Markov process using the concept of sojourn time [3].

2.1. Multi-State Model and Transition Rates

The state transition model [2] that was selected as a case-study for passive component degradation involves six ordinary differential equations which are solved by a semi-Markov approach to account for system history and local thermal operating condition-dependent transition rates [3,4]. Fig. 1 shows the Markov model states for the crack initiation and growth. State evolutions are described through

$$dS/dt = -\phi_1 S + \omega_1 M + \omega_2 D + \omega_3 C + \omega_4 L \quad (1)$$

$$dM/dt = \phi_1 S - \omega_1 M - \phi_2 M - \phi_3 M \quad (2)$$

$$dC/dt = \phi_3 M - \omega_3 C - \phi_6 C \quad (3)$$

$$dD/dt = \phi_2 M - \omega_2 D - \phi_4 D \quad (4)$$

$$dL/dt = \phi_4 D - \omega_4 L - \phi_5 L \quad (5)$$

$$dR/dt = \phi_6 C + \phi_5 L \quad (6)$$

where *S(t), M(t), C(t), D(t), L(t), R(t)* denote the probability of being in the states shown in Fig.1 at time *t*. The transition rates ϕ_5, ϕ_6 and repair rates ω_i (i=1, 2, 3) are constant. Other transition and repair rates in Eqs.(1)-(6) are as defined below

ω_1 : Repair transition rate from micro-crack
ω_2 : Repair transition rate from radial macro-crack
ω_3 : Repair transition rate from circumferential macro-crack
ω_4 : Repair transition rate from leak
$\emptyset_5$: Leak to rupture transition rate
$\emptyset_6$: Macro-crack to rupture transition rate

A simplified model of the transition rates $\phi_i(t)$ (i=1,…,4) as presented in [2] are as follow:

$$\phi_1(t) = (b/\beta)(t/\beta)^{b-1} \quad (7)$$

$$\phi_2(t) = \begin{cases} 0 & \text{if } u \le \frac{a_D}{\dot{a}_M} \\ a_D P_D/(u\, a_D P_D + u^2\, \dot{a}_M P_c) & \text{if } u > a_D/\dot{a}_M \text{ and } u \le a_C/\dot{a}_M \\ \frac{a_D P_D}{u\, a_D P_D + u\, a_C P_c} & \text{if } u > \frac{a_D}{\dot{a}_M} \text{ and } u > a_C/\dot{a}_M \end{cases} \quad (8)$$

$$\phi_3(t) = \begin{cases} 0 & \text{if } u \le \frac{a_C}{\dot{a}_M} \\ a_C P_C/(u\, a_D P_D + u^2\, \dot{a}_M P_C) & \text{if } u > a_C/\dot{a}_M \text{ and } u \le a_D/\dot{a}_M \\ \frac{a_C P_C}{u\, a_D P_D + u\, a_C P_C} & \text{if } u > \frac{a_C}{\dot{a}_M} \text{ and } u > a_D/\dot{a}_M \end{cases} \quad (9)$$

$$\phi_4(t) = \begin{cases} 1/w & \text{if } w > (a_L - a_D)/\dot{a}_M \\ 0 & \text{otherwise} \end{cases} \quad (10)$$

In Eqs.(8) - (10), u is a time after crack initiation and w is time after macro-crack formation (see Fig.1). The other parameters in Eqs.(7) - (10) are the following

a_D : Crack length threshold for radial macro-crack
P_D : Probability that micro-crack evolves as radial crack
a_C : Crack length threshold for circumferential macro-crack
P_C : Probability that micro-crack evolves as circumferential crack
a_L : Crack length threshold for leak

Figure 1: Multi-state transition model for PWSCC [2].

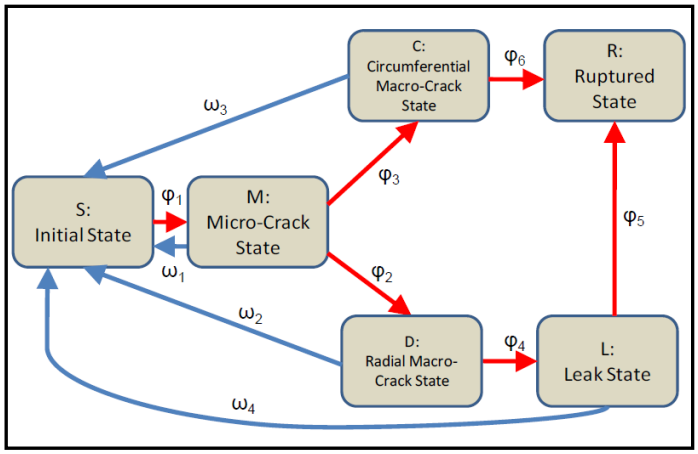

2.1.1. Crack Initiation and Growth Rate Equations

Of the alternative models that have been used to characterize initiation, the Weibull model is the most widely adopted [6] in which the cumulative probability $P(t)$ of crack initiation by time t is quantified through,

$$P(t) = 1 - e^{(t/\tau)b} \quad (11)$$

$$\tau = A\sigma^n e^{(Q/RT)} \quad (12)$$

where

b : Weibull shape parameter for crack initiation model
τ : Weibull scale parameter for crack initiation model
A : Fitting parameter
σ : Explicit stress factor
n : Stress exponent factor

Q : Crack initiation activation energy
T : Absolute temperature at crack location
R : The universal gas constant.

Table 1 below defines the units for the variables in Eqs.(11) and (12), as well as their values/distributions as used in different studies. Base case values refer to the data which were used in [3].

Table 1: Definition of the Inputs in Crack Initiation Model

Crack Initiation (Weibull Model) Inputs						
Symbol	**Unit**	**Value**				
		xLPR [7]		**Unwin[8]**		**Base Case [3]**
T	K	Distribution Type	Normal	617		610
		Mean	617.9			
		Std. Deviation	0.0882			
		Deterministic	618			
b	ND	3		Distribution Type	Triangular	2
				Minimum	3.915	
				Mode	4.35	
				Maximum	4.785	
σ	MPa	Distribution Type	Normal	Distribution Type	Normal	106
		Mean	300.3	Mean	300.3	
		Std. Deviation	110	Std. Deviation	110	
		Deterministic	150	Deterministic	150	
n	ND	-4		Distribution Type	Triangular	-7
				Minimum	-7.7	
				Mode	-7	
				Maximum	-6.3	
A	ND	0.04		2.524×10^5		2.524×10^5
Q_I	kJ/mole	182.908		Distribution Type	Triangular	130
				Minimum	116.73	
				Mode	129.7	
				Maximum	142.67	

The maximum crack growth rate, $\dot{a_M}$, (see Eqs. 8-10) is calculated by using MRP-115 Model [9]

$$\dot{a}_M = \alpha f_{alloy} f_{orient} K^{\beta} e^{-\left(\left(\frac{Q_G}{R}\right)(T^{-1}-(T_{ref})^{-1})\right)} \quad (13)$$

where

α : Fitting constant – crack growth amplitude
T : Absolute operating temperature at crack location
T_{ref} : Absolute reference temperature used to normalize data (598.15 K)
Q_G : Thermal activation energy for crack growth
R : The universal gas constant
K : Crack tip stress intensity factor
f_{alloy} : 1.0 for Alloy 182 and 1/2.6 for Alloy 82
f_{orient} : 1.0, except 0.5 for crack propagation that is perpendicular to dendrite solidification direction.
β : Stress intensity exponent

Table 2 below defines the units for the variables in Eq.(13) as well as their values/distributions as used in different studies.

Table 2: Definition of the Inputs in Crack Growth Model

Crack Growth (MRP-115) Model Inputs						
Symbol	**Unit**	**Value**				
		xLPR [7]		**Unwin [8]**		**Base Case[3]**
β	ND	1.6		Distribution Type	Triangular	1.6
				Minimum	1.44	
				Mode	1.6	
				Maximum	1.76	
α	(m/s) $(MPa\text{-}m^{0.5})^{1.6}$	9.82×10^{-13}		Distribution Type	Normal	1.5×10^{-12}
				Threshold	-	
				Mean	8×10^{-13}	
				Std. Deviation	-	
Q_G	kJ/mole	Distribution Type	Normal	Distribution Type	Normal	130
		Mean	130	Mean	130	
		Std. Deviation	5	Std. Deviation	5	
		Deterministic	130	Deterministic	130	
f_{alloy}	ND	Distribution Type	Lognormal	1.0		1.0
		Mean	0.99894			
		Std. Deviation	1.83475			
		Deterministic	1.074897			
f_{orient}	ND	1.0		1.0		1.0

2.2. Sojourn Time Approach

The variables *u* and *w* in Eqs.(8)- (10) represent the residence time of the system in States M and C or D, respectively (see Fig.1). In that respect, Eqs.(1)-(10) do not have the Markov property of being independent of state history. These equations are converted into a semi-Markov process using the sojourn (or expected residence) time approach determined through

$$\frac{d\tau_{n,k}(t)}{dt} = (t - T_{k-1})\left[-x_n(t)\sum_{\substack{m=1 \\ m\neq n}}^{N}\phi_{mn}(\tau_n) + \sum_{\substack{m=1 \\ m\neq n}}^{N}\phi_{nm}(\tau_m)\,x_m(t)\right] \qquad (14)$$

where $\tau_{n,k}(t)$ is sojourn time of state *n* and for *kth* time interval, $x_n(t)$ is the probability of being in State *n* at time *t*, and $\phi_{nm}(\tau_m)$is the transition rate from State *n* to State *m* as a function of sojourn time.

A sensitivity analysis of the aging model on local thermal operating conditions has been performed [4] since the transition rates $\phi_1(t)$ through $\phi_4(t)$ in Eqs.(7)-(10), respectively, are affected by the thermal-hydraulic conditions as they affect the time constant. Thermal-hydraulic data for this analysis have been obtained using the transient code RELAP/SCDAMSIM [10] for a simplified model of a four loop PWR.

3. QUANTIFYING UNCERTAINTY FOR THE STATE TRANSITION MODEL

As indicated in Tables 1 and 2, the multi-state transition model described in Section 2 is subject to considerable uncertainty and/or variability in both initial conditions and parameters. Most numerical approaches address such challenges by: a) computing local sensitivity indices (partial derivatives of the solution with respect to the input variables) [11], b) solving the model for a statistically large ensemble of random or quasi-random input values [12-14], or, c) by approximating the functional relationship of the input and output [15-17]. In this paper, Option (b) is used for uncertainty analysis, and Option (c) is used for sensitivity analysis, as described in Sections 3.1 and 3.2, respectively.

3.1. Uncertainty Analysis

Several random variable sampling techniques are employed in the literature [7], such as random sampling, Latin hypercube sampling (LHS), and discrete probability distribution (DPD) sampling schemes. The output of interest is the probability of rupture, which is expected to be extremely low for primary piping systems. Therefore random sampling may generate many runs without any rupture. In such a situation, a common strategy is to use Latin hypercube sampling to propagate the effects of aleatory uncertainty [12].

In this study, all parameters in Eqs.(1)-(13) except T and σ are treated as invariant. The T and σ were assigned uncertainty distributions based on the results of a preliminary sensitivity screening process among the parameters T, σ, n, b, Q_G and α in Eqs.(11)-(13) to identify those with the most significant effect on rupture probability.

In the initial analysis, temperature T and residual weld stress σ were importance sampled without distinguishing between epistemic and aleatory uncertainties. Confidence levels on the output variables were estimated as a function of time. The estimation was accomplished by computing the 95^{th} and 5^{th} percentiles of the distribution on the probability of leak $L(t)$ and rupture $R(t)$ at each time point. Figure 2 shows the results of this one-step uncertainty analysis with the 95^{th} (red line) and 5^{th} (blue line) percentiles.

As indicated in the xLPR study [7], when it is possible to differentiate between aleatory and epistemic uncertainties in a model, additional information can be obtained that could affect the interpretation of results by performing a two-loop simulation in which the inner loop and outer loop address the aleatory uncertainties and the epistemic uncertainties, respectively. In the outer loop, parameter values are sampled from epistemic uncertainty distributions and passed on to the inner loop. For each sample in the outer loop, LHS draws from aleatory uncertainty distributions are performed in the inner loop over the time-frame of interest accounting for the aleatory uncertainty. From these results an average rupture probability can be calculated over the variability associated with the input parameters. From the outer loop analysis, it is therefore possible to obtain an uncertainty distribution of the variability-averaged rupture probabilities. This distribution provides measures of the uncertainty in rupture probability that could be reduced by further experimentation or model development. As LHS is also used to generate epistemic uncertainty, the simple arithmetic mean of the rupture probability over epistemic uncertainty can be used to estimate an over-all expected value $\langle R \rangle$ of the rupture probability from

$$\langle R \rangle = \frac{1}{N}\sum_{n=1}^{N}\left(\frac{1}{M}\sum_{m=1}^{M} R_{mn}\right) \quad (15)$$

where M is the number of aleatory draws, N is the number of epistemic draws and R_{mn} are the rupture probabilities calculated from the state transition model for each draw combination. In general, it is expected that the overall average value will be the same regardless of whether the sampling is performed in a single-step or a two-step process. However, to test whether the overall average is affected by the sampling approach, a comparison was made of the two-step LHS versus single step LHS. Uncertainty in T and σ were characterized using normal PDFs: $T \sim$ Normal (617.9, 0.0882), $\sigma \sim$

Normal (300.3, 30)) for both cases. In the two-step LHS, the uncertainty for T and σ were characterized as epistemic and aleatory, respectively, instead of both as epistemic. Equation (15) was implemented with N=100 and M=100 resulting in a total of 10,000 realizations. The single step LHS realization was also performed for 10,000 draws to obtain $\langle R \rangle$. Fig. 3 shows the comparison of single step and two-step LHS sampling processes and Fig. 4 shows $\langle R \rangle$ as a function of time for the single-step and two-step LHS. The temperature draws T_N in Fig. 3 are for every 2 years. As can be seen in Fig. 4, difference between two methods is extremely small (on the order of 10^{-5}).

Figure 2: Leak (L) and Rupture (R) probabilities of PWR pressurizer surge line pipe (Alloy 182) for a PWSCC scenario over 80 years. The red line indicates 95th and blue line indicates 5th percentile.

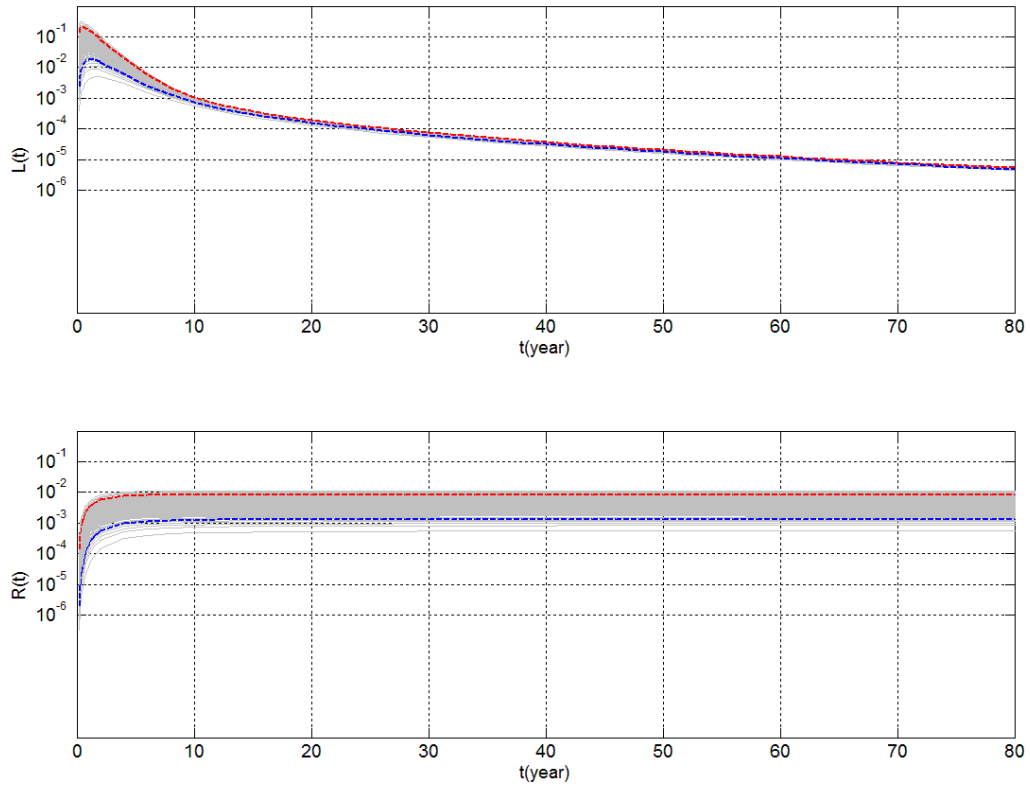

3.2. Sensitivity Analyses

In order to determine whether T or σ had more impact on the rupture probability, a response surface approach was used. The fitting was done by using the method of least squares and a second order fitting using

$$f(T,\sigma) = p_{00} + p_{10}T + p_{01}\sigma + p_{20}T^2 + p_{11}T\sigma + p_{02}\sigma^2 \qquad (16)$$

Coefficients of Eq. (16) are listed in Table 3 and statistics goodness-of-fit data are summarized in Table 4.

Figure 3: Illustration of single step and two-step LHS comparisons

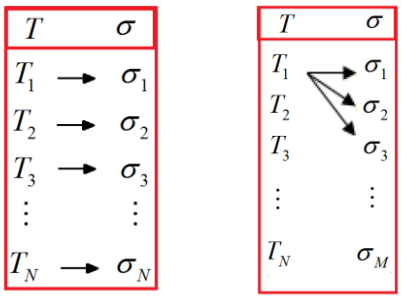

a. Single Step LHS **b. Two-Step LHS**

As can be seen in Fig. 4, difference between two methods is extremely small (on the order of 10^{-5}).

Figure 4: Illustration of single step and two-step LHS comparisons

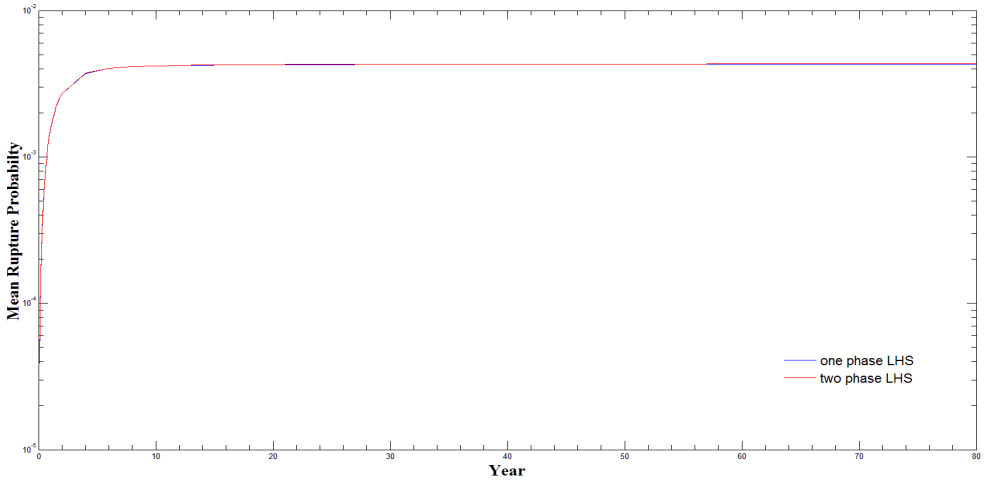

Table 3: Fitting equation coefficients and 95% confidence bounds

Coefficients	95% confidence bounds
p_{00} = -24.39	-363.2, 314.5
p_{10} = -7.953 x10^{-5}	-0.003004, 0.002845
p_{01} = 0.07899	-1.017, 1.175
p_{20} = 3.302 x10^{-7}	3.228 x10^{-7}, 3.375 x10^{-7}
p_{11} = -7.747 x10^{-8}	-4.81 x10^{-6}, 4.655 x10^{-6}
p_{02} = -6.394 x10^{-5}	-9.51 x10^{-5}, 8.231 x10^{-4}

Table 4: Statistic goodness-of-fit data

Goodness of fit
SSE: 2.457 x10^{-7}
R-square: 0.9995
Adjusted R-square: 0.9995
RMSE: 5.113 x10^{-5}

Fig. 5 shows the impact of weld residual stress and temperature variations on the rupture probability at t=40 years in case of 100 realizations and clearly indicates greater sensitivity of rupture probability to the uncertainty in stress than to the uncertainty in temperature.

Figure 5: Response Surface of Rupture Probability

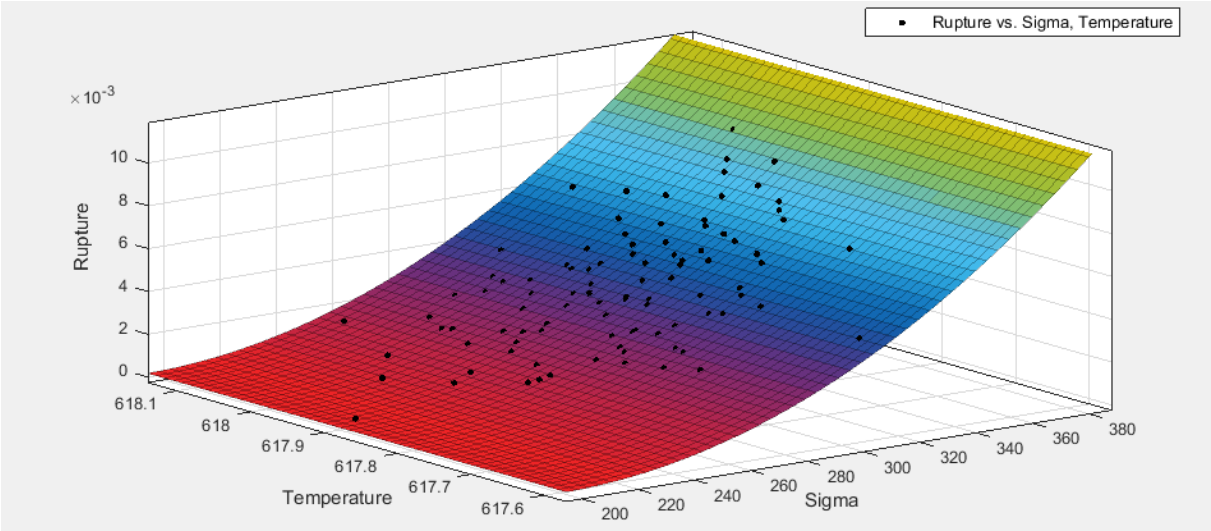

4. CONCLUSION

Using a state-transition model to describe (PWSCC), uncertainties in the input data for crack initiation and crack growth are represented by probability distributions. LHS is used to generate observations from the distributions governing T and σ with a two-step approach that distinguishes between aleatory and epistemic uncertainties. Comparison of the results to a single-step quantification process indicates that the differences between one-step and two-step approach are negligible with regard to the mean rupture probability (on the order of 10^{-5}). However, the separation into sources of aleatory and epistemic uncertainty could enable the decision-maker to determine the potential value of activities to reduce the epistemic uncertainty, such as by the performance of research. Indeed, for this example, nearly all of the uncertainty shown in Fig. 2 arises from the "epistemic" uncertainty associated with the weld residual stress σ.

Acknowledgements

This research has been performed using funding received from the DOE Office of Nuclear Energy's Nuclear Energy University Programs.

References

[1] R. Lewandowski, R. Denning, T. Aldemir, J. Zhang, *"Development of a Living, Plant-Condition Dependent Probabilistic Safety Assessment,"* these proceedings.

[2] S. D. Unwin, P.P. Lowry, R.F. Layton Jr., P. G. Heasler, and M. B. Toloczko, "*Multi-State Physics Models of Aging Passive Components in Probabilistic Risk Assessment*," ANS PSA 2011 International Topical Meeting on Probabilistic Safety Assessment and Analysis, Wilmington, NC, (2011).

[3] A. Guler, T. Aldemir, R. Denning, *"The Sojourn Time Approach for Modeling Aging in Passive Components,"* Trans. Am. Nucl. Soc., 108, pp. 552-554, (2013).

[4] A. Guler, T. Aldemir, R. Denning, *"Multi-State Physics Based Aging Assessment of Passive Components,"* Proc. ANS PSA 2013 International Topical Meeting on Probabilistic Safety Assessment and Analysis, Columbia, SC, (2013).

[5] K. Fleming, *"Markov models for evaluating risk-informed in-service inspection strategies for nuclear power plant piping systems,"* Reliability Engineering and System Safety, 83, pp. 27–45, (2004).

[6] W.J. Shack and O.K. Chopra, *"Statistical Initiation and Crack Growth Models for Stress Corrosion Cracking,"* Proceedings of the ASME Pressure Vessels and Piping Conference (PVP2007), San Antonio, Texas, July 22–26, 2007, pp. 337-344, (2007).

[7] P.D. Mattie, D.A. Kalinich, C.J. Sallaberry, U.S. Nuclear Regulatory Commission, *"Extremely Low Probability of Rupture Pilot Study: xLPR Framework Model User's Guide"*, SAND2010-7131, Sandia National Laboratories, Albuquerque, New Mexico, (2010).

[8] S.D. Unwin, K.I. Johnson and P.W. Eslinger, *"Robustness of RISMC Insights under Alternative Aleatory/Epistemic Uncertainty Classifications,"* Draft Report PNNL-21810, Pacific Northwest National Laboratory, Richland, WA, (2012).

[9] Electric Power Research Institute, *"Materials Reliability Program Crack Growth Rates for Evaluating Primary Water Stress Corrosion Cracking of Alloy 82,182, and 132 Welds,"* EPRI Report MRP-115, 1006696, Palo Alto, CA (2003).

[10] SCDAP/RELAP5 Development Team, *"SCDAP/RELAP5/MOD3.2 Code Manual, Vol. 1–5,"* NUREG/CR-6150, INEL-96/0422, (1998).

[11] T. Turányi, *"Sensitivity Analysis of Complex Kinetic Systems. Tools and Applications*," J Math Chem, 5, pp. 203-248, (1990).

[12] J.C. Helton, F.J. Davis, *"Latin hypercube sampling and the propagation of uncertainty in analyses of complex systems,"* Reliability Engineering and System Safety, 81, pp. 23–69, (2003).

[13] S. Marino et al., *"A methodology for performing global uncertainty and sensitivity analysis in systems biology."* J Theor Biol., 254, pp. 178-196, (2008).

[14] C.P. Robert, G. Casella, *"Monte Carlo statistical methods,"* New York: Springer, (2004).

[15] S. Fang et al., *"Improved generalized Fourier amplitude sensitivity test (FAST) for model assessment,"* Statist Comput, 13, pp. 221-226, (2003).

[16] W.J. Hill, W.G. Hunter, *"A Review of Response Surface Methodology: A Literature Survey,"* Technometrics, 8, pp. 571-590, (1966).

[17] A.I. Khuri., *"Response Surface Methodology and Related Topics,"* Singapore, World Scientific Publishing Co, (2006).